

# Higgs-mediated enhancement of interlayer transport in high- $T_c$ superconductors

Guido Homann,<sup>1</sup> Jayson G. Cosme,<sup>1,2,3</sup> Junichi Okamoto,<sup>4,5</sup> and Ludwig Mathey<sup>1,2</sup>

<sup>1</sup>*Zentrum für Optische Quantentechnologien and Institut für Laserphysik, Universität Hamburg, 22761 Hamburg, Germany*

<sup>2</sup>*The Hamburg Centre for Ultrafast Imaging, Luruper Chaussee 149, 22761 Hamburg, Germany*

<sup>3</sup>*National Institute of Physics, University of the Philippines, Diliman, Quezon City 1101, Philippines*

<sup>4</sup>*Institute of Physics, University of Freiburg, Hermann-Herder-Strasse 3, 79104 Freiburg, Germany*

<sup>5</sup>*EUCOR Centre for Quantum Science and Quantum Computing, University of Freiburg, Hermann-Herder-Strasse 3, 79104 Freiburg, Germany*

(Dated: January 19, 2022)

We put forth a mechanism for enhancing the interlayer transport in cuprate superconductors, by optically driving plasmonic excitations with a frequency that is blue-detuned from the Higgs frequency. The plasmonic excitations induce a collective oscillation of the Higgs field which induces parametric enhancement of the superconducting response, as we demonstrate with a minimal analytical model. Furthermore, we perform relativistic  $U(1)$  lattice gauge simulations and find good agreement with our analytical prediction. We map out the renormalization of the interlayer coupling as a function of the parameters of the optical field and demonstrate that the Higgs-mediated enhancement can be larger than 50%.

The observation of light-induced superconductivity in cuprates and organic salts has been associated with exciting lattice or molecular vibrations [1–3]. Related experiments on light-enhanced interlayer transport in the bilayer cuprate YBCO above and below the critical temperature  $T_c$  have been reported in [4–7]. Several mechanisms for these observations have been proposed in [8–14]. These proposed mechanisms focus on inducing phononic motion and its influence on the superconducting response. Here, we propose to enhance the interlayer transport in cuprates by optically exciting Higgs oscillations. This collective motion of the Higgs field couples parametrically to the plasma field, which results in the enhancement of the superconducting response. Our primary example will be monolayer cuprates. We expect that similar results emerge for other lattice geometries as well. We demonstrate that the enhancement of the superconducting response, in particular the low-frequency behavior of the imaginary conductivity, is achieved for driving frequencies that are slightly blue-detuned from the Higgs frequency. Thus, we expand the scope of dynamical control of the superconducting state in the cuprates by exploiting nonlinear plasmonics [15, 16].

In this Letter, we first consider a two-mode model with a cubic coupling of the Higgs and plasma modes [17]. Based on this minimal model, we provide an analytical expression for the Higgs-mediated renormalization of the interlayer coupling in monolayer cuprates. We then extend our treatment to a relativistic  $U(1)$  lattice gauge theory and simulate the  $c$ -axis optical conductivity for different ratios of the Higgs and plasma frequencies at zero temperature. The numerical results confirm our analytical prediction, and we identify the optimal parameter regime for observing the enhancement effect.

Expanding on previous works [18–21], we model a layered superconductor as a stack of intrinsic Josephson junctions. In addition to Josephson plasma resonances

[22–24], recent experiments have revealed the existence of another fundamental excitation in cuprate superconductors, the Higgs mode [25–27]. This mode corresponds to amplitude oscillations of the superconducting order parameter  $\psi$ , which decouples from the plasma mode

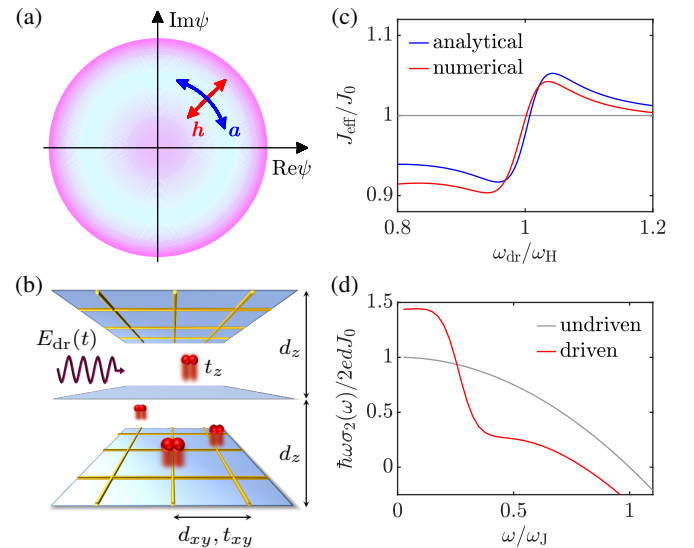


FIG. 1. (a) Higgs and plasma modes of a monolayer cuprate superconductor, illustrated with a Mexican hat potential for the superconducting order parameter. (b) Schematic representation of a layered superconductor periodically driven by an electric field with frequency  $\omega_{dr}$  and field strength  $E_0$ . (c) Effective interlayer coupling  $J_{\text{eff}}$  rescaled by its equilibrium value  $J_0$  at  $T = 0$ . The field strength is fixed at  $E_0 = 100 \text{ kV cm}^{-1}$ . (d) Numerical results for the imaginary conductivity  $\sigma_2$  at  $T = 0$ . The driving parameters are  $\omega_{dr} = 1.05 \omega_H$  and  $E_0 = 400 \text{ kV cm}^{-1}$ . The monolayer system considered in (c) and (d) has the Josephson plasma frequency  $\omega_J/2\pi = 2 \text{ THz}$  and the Higgs frequency  $\omega_H/2\pi = 6 \text{ THz}$ .

for a system with approximate particle-hole symmetry [28, 29]. The two distinct low-energy modes of a monolayer cuprate superconductor are depicted in Fig. 1(a), where the phase of  $\psi$  shall be interpreted as the gauge-invariant phase difference between adjacent layers. At zero momentum, the lowest-order coupling between the Higgs field  $h$  and the unitless vector potential  $a$  is given by the cubic interaction Lagrangian  $\mathcal{L}_{\text{int}} \sim a^2 h$  [27, 30]. The equations of motion corresponding to such a minimal model for describing the dynamics of a light-driven monolayer cuprate at zero temperature are

$$\ddot{h} + \gamma \dot{h} + \omega_H^2 h + \alpha \omega_J^2 a^2 = 0, \quad (1)$$

$$\ddot{a} + \gamma \dot{a} + \omega_J^2 a + 2\omega_J^2 a h = j, \quad (2)$$

where  $\omega_H$  is the Higgs frequency,  $\omega_J$  is the plasma frequency,  $\gamma$  is the damping constant, and  $\alpha$  is the capacitive coupling constant of the junctions. The interlayer

current  $j$  is induced by an external electric field. We use  $\gamma/2\pi = 0.5$  THz and  $\alpha = 1$  throughout this Letter, and we assume the  $z$  axis to be aligned with the  $c$  axis of the crystal.

For weak pump-probe strengths, we perform a perturbative expansion for  $a$  and  $h$  around their equilibrium values. To calculate the  $c$ -axis optical conductivity  $\sigma(\omega) = J_z(\omega)/E_z(\omega)$ , we apply a current with both driving and probing terms, i.e.,  $j = j_{\text{dr}} e^{-i\omega_{\text{dr}} t} + j_{\text{pr}} e^{-i\omega_{\text{pr}} t} + \text{c.c.}$ . We take the current as a first order term in the expansion such that the leading contribution to  $a$  is of first order. Hence, the leading contribution to  $h$  is of second order, and the coupling term  $\sim ah$  gives a third order correction to  $a$ . Additionally, we assume that the probing frequency  $\omega_{\text{pr}}$  is much smaller than the driving frequency  $\omega_{\text{dr}}$ . Thus, we obtain an approximate analytical prediction [31] for the conductivity given by

$$\omega_{\text{pr}} \sigma(\omega_{\text{pr}}) = \frac{i\epsilon_z \epsilon_0 j(\omega_{\text{pr}})}{a(\omega_{\text{pr}})} \approx \frac{i\epsilon_z \epsilon_0 \omega_J^2 \omega_H^2 (\omega_{\text{dr}}^2 - \omega_H^2 + i\gamma\omega_{\text{dr}}) [(\omega_{\text{dr}}^2 - \omega_J^2)^2 + \gamma^2 \omega_{\text{dr}}^2]}{\omega_H^2 (\omega_{\text{dr}}^2 - \omega_H^2 + i\gamma\omega_{\text{dr}}) [(\omega_{\text{dr}}^2 - \omega_J^2)^2 + \gamma^2 \omega_{\text{dr}}^2] + 4\alpha \omega_J^2 |j_{\text{dr}}|^2 (\omega_{\text{dr}}^2 - 3\omega_H^2 + i\gamma\omega_{\text{dr}})}. \quad (3)$$

where  $\epsilon_z$  denotes the dielectric permittivity of the junctions, and  $j_{\text{dr}}$  is the driving amplitude. We define an effective Josephson coupling [13] based on the  $1/\omega$  divergence of the conductivity:

$$J_{\text{eff}} = \frac{\hbar}{2ed_z} \text{Im}[\omega_{\text{pr}} \sigma(\omega_{\text{pr}})]_{\omega_{\text{pr}} \rightarrow 0}, \quad (4)$$

with the interlayer spacing  $d_z$ . In the absence of driving, the Josephson coupling is  $J_0 = \hbar\epsilon_z\epsilon_0\omega_J^2/(2ed_z)$  according to Eq. (3). The analytical prediction for  $J_{\text{eff}}/J_0$  in the presence of driving is shown in Fig. 1(c). The key result of this work is the enhancement of the effective interlayer coupling when the pump frequency is slightly blue-detuned from the Higgs frequency. This enhancement phenomenon is due to parametric amplification. Indeed, Eq. (2) takes the form of a parametric oscillator due to the two-wave mixing of drive and probe in Eq. (1), inducing amplitude oscillations at frequencies  $2\omega_{\text{dr}}$ ,  $2\omega_{\text{pr}}$ , and  $\omega_{\text{dr}} \pm \omega_{\text{pr}}$ . The coupling of amplitude oscillations with  $\omega_{\text{dr}} \pm \omega_{\text{pr}}$  to the drive amplifies the current response at the probing frequency. The numerical results in Figs. 1(c) and 1(d), further highlighting the enhancement of interlayer transport, are obtained by simulating a full lattice gauge model discussed in the following.

We now turn to our relativistic  $U(1)$  lattice gauge theory in three dimensions, where the layered structure of cuprate superconductors is encoded in the lattice parameters. Our approach allows us to explicitly simulate the coupled dynamics of the order parameter of the superconducting state  $\psi_{\mathbf{r}}(t)$  and the electromagnetic field  $\mathbf{A}_{\mathbf{r}}(t)$

at temperatures below  $T_c$ . To this end, we describe the Cooper pairs as a condensate of interacting bosons with charge  $-2e$ , represented by the complex field  $\psi_{\mathbf{r}}(t)$ . The time-independent part of our model Lagrangian has the form of the Ginzburg-Landau free energy [32], discretized on an anisotropic lattice. We model the layered structure of high- $T_c$  cuprates using an anisotropic lattice geometry as illustrated in Fig. 1(b). The discretization length  $d_{xy}$  constitutes a short-range cutoff around the in-plane coherence length, while the interlayer spacing  $d_z$  is the distance between the  $\text{CuO}_2$  planes in the crystal. Each component of the vector potential  $A_{s,\mathbf{r}}(t)$  is located at half a lattice site from site  $\mathbf{r}$  in the  $s$  direction, where  $s \in \{x, y, z\}$ . According to the Peierls substitution, it describes the averaged electric field along the bond of a plaquette in Fig. 1(b).

We discretize space by mapping it on a lattice and implement the compact  $U(1)$  lattice gauge theory in the time continuum limit [33]. The Lagrangian of the lattice gauge model is

$$\mathcal{L} = \mathcal{L}_{\text{sc}} + \mathcal{L}_{\text{em}} + \mathcal{L}_{\text{kin}}. \quad (5)$$

The first term is the  $|\psi|^4$  model of the superconducting condensate in the absence of Cooper pair tunneling:

$$\mathcal{L}_{\text{sc}} = \sum_{\mathbf{r}} K \hbar^2 |\partial_t \psi_{\mathbf{r}}|^2 + \mu |\psi_{\mathbf{r}}|^2 - \frac{g}{2} |\psi_{\mathbf{r}}|^4, \quad (6)$$

where  $\mu$  is the chemical potential, and  $g$  is the interaction strength. This Lagrangian is particle-hole symmetric due

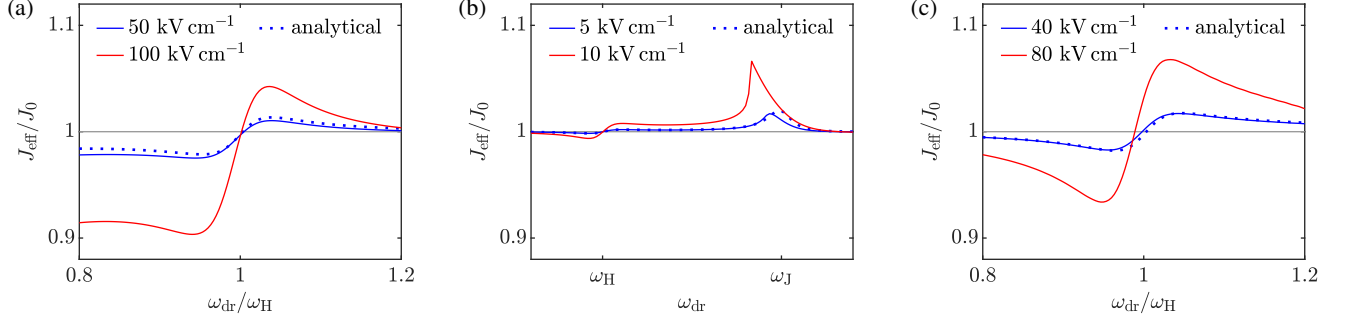


FIG. 2. Effective interlayer coupling for three light-driven monolayer cuprate superconductors with different ratios  $\omega_J/\omega_H$ . (a)  $\omega_J < \omega_H$ , (b)  $\omega_H < \omega_J < \sqrt{3}\omega_H$ , (c)  $\sqrt{3}\omega_H < \omega_J$ . Each panel shows the dependence on the driving frequency  $\omega_{dr}$  for two fixed values of the field strength  $E_0$  at  $T = 0$ . Solid lines correspond to numerical results, dotted lines indicate analytical results for the lower field strength. In all cases, the Higgs frequency is fixed at  $\omega_H/2\pi = 6$  THz, while the plasma frequency  $\omega_J/2\pi$  is varied: (a) 2 THz, (b) 9 THz, and (c) 16 THz.

to its invariance under  $\psi_{\mathbf{r}} \rightarrow \psi_{\mathbf{r}}^*$ . The coefficient  $K$  describes the magnitude of the dynamical term [27, 29].

The electromagnetic part  $\mathcal{L}_{em}$  is the discretized form of the free-field Lagrangian:

$$\mathcal{L}_{em} = \sum_{s,\mathbf{r}} \frac{\epsilon_s \epsilon_0}{2} E_{s,\mathbf{r}}^2 - \frac{1}{\mu_0 \beta_s^2} \left[ 1 - \cos(\beta_s B_{s,\mathbf{r}}) \right]. \quad (7)$$

Here  $E_{s,\mathbf{r}}$  denotes the  $s$  component of the electric field, and the magnetic field components  $B_{s,\mathbf{r}}$  follow from the finite-difference representation of  $\nabla \times \mathbf{A}$ . The temporal and spatial arrangement of the electromagnetic field is consistent with the finite-difference time-domain (FDTD) method for solving Maxwell's equations [34]. Note that we choose the temporal gauge for our calculations, i.e.,  $E_{s,\mathbf{r}} = -\partial_t A_{s,\mathbf{r}}$ . The dielectric permittivities are  $\epsilon_x = \epsilon_y = 1$  and  $\epsilon_z = 4$ . The coefficients for the magnetic field are  $\beta_x = \beta_y = 2ed_{xy}d_z/\hbar$  and  $\beta_z = 2ed_{xy}^2/\hbar$ .

The nonlinear coupling between the Higgs field and the electromagnetic field derives from the tunneling term

$$\mathcal{L}_{kin} = - \sum_{s,\mathbf{r}} t_s |\psi_{\mathbf{r}'(s)} - \psi_{\mathbf{r}} e^{ia_{s,\mathbf{r}}}|^2, \quad (8)$$

where  $\mathbf{r}'(s)$  denotes the neighboring lattice site of  $\mathbf{r}$  in the  $s$  direction. The unitless vector potential  $a_{s,\mathbf{r}} = -2ed_s A_{s,\mathbf{r}}/\hbar$  couples to the phase of the superconducting field, ensuring the local gauge-invariance of  $\mathcal{L}_{kin}$ . The in-plane tunneling coefficient is  $t_{xy}$ , and the interlayer tunneling coefficient is  $t_z$ .

We numerically solve the equations of motion derived from the Lagrangian, employing periodic boundary conditions. We integrate the differential equations using Heun's method with step size  $\Delta t = 2.5$  as. Here, we restrict ourselves to zero temperature, where the in-plane dynamics is silent. The finite-temperature case including dissipation and Langevin noise [17] will be discussed elsewhere.

We drive the system by adding  $-\omega_{dr} E_0 \sin(\omega_{dr} t)$  to the equations of motion for the electric field component  $E_{z,\mathbf{r}}(t)$ , which describes a spatially homogeneous driving field. Note that Eqs. (1) and (2) can be derived as the Euler-Lagrange equations of the Lagrangian (5), assuming that the superconducting order parameter is uniform across the entire sample. To recover Eqs. (1) and (2), one neglects interaction terms in  $\mathcal{L}_{sc}$  beyond quadratic order and coupling terms in  $\mathcal{L}_{kin}$  beyond cubic order. The Higgs field is given by  $h = |\psi|/|\psi_0| - 1$ , where  $|\psi_0| = \sqrt{\mu/g}$  is the equilibrium condensate amplitude. The plasma and Higgs frequencies can be expressed as  $\omega_J = \sqrt{t_z/\alpha K \hbar^2}$  and  $\omega_H = \sqrt{2\mu/K \hbar^2}$ , respectively. The drive induces a current with amplitude  $|j_{dr}| = ed_z \omega_{dr} E_0 / \hbar \epsilon_z$ .

In the following, we present our numerical results. We evaluate the effective interlayer coupling based on the optical conductivity at  $\omega_{pr} = \omega_H/120$ . For weak driving, we find decent agreement between the analytical prediction in Eq. (3) and the numerical results of the full lattice gauge model, as shown in Fig. 2. The deviations are due to higher-order terms ignored in the minimal model and the perturbative expansion. They grow with increasing field strength. Nevertheless, our simulations demonstrate that the enhancement effect persists for strong driving, even in the presence of higher-order nonlinearities, fully included in our  $U(1)$  lattice gauge theory.

We find that the renormalization of the interlayer coupling does not only depend on the driving parameters, but also on the ratio of the Higgs frequency and the plasma frequency of the system. Our main proposal consists of driving the superconductor slightly blue-detuned from the Higgs frequency  $\omega_H$ . This mechanism is effective for all ratios of  $\omega_J/\omega_H$ . As we discuss below, there is a second regime in which dynamical stabilization can be achieved, if the system fulfills the requirement  $\omega_H < \omega_J < \sqrt{3}\omega_H$ .

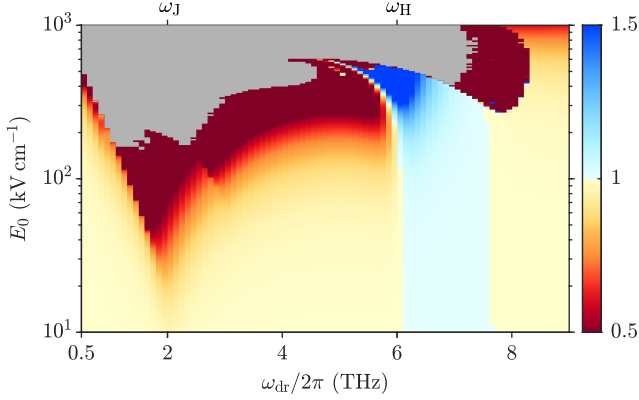


FIG. 3. Dependence of the effective interlayer coupling  $J_{\text{eff}}/J_0$  on the driving frequency  $\omega_{\text{dr}}$  and the field strength  $E_0$  at  $T = 0$ . The gray area marks the heating regime.

Figure 3 displays the renormalized interlayer coupling as a function of the driving parameters for a monolayer cuprate with  $\omega_J < \omega_H$ . Consistent with our analytical prediction, the interlayer transport is enhanced for driving frequencies blue-detuned from the Higgs frequency, while it is diminished on the red-detuned side, as immediately apparent for weak driving. In general, higher field strengths amplify the suppression/enhancement effects and additionally renormalize the Higgs frequency and the plasma frequency. The frequency renormalization of the Higgs mode results in the bending of the enhancement regime towards lower driving frequencies for larger driving fields. This observation reflects the general behavior of nonlinear oscillators to display amplitude-dependent eigenfrequencies [35]. We emphasize that the interlayer coupling can be increased by more than 50%, for this example. The strongest suppression of interlayer transport occurs for driving close to the plasma frequency. This is generally the case if  $\omega_J < \omega_H$  or  $\omega_J > \sqrt{3}\omega_H$ .

The enhancement and suppression effects are limited by heating that dominates for larger field strengths, see also Ref. [17]. Here we identify the heating regime based on the condition that the condensate becomes completely depleted at some instant of time. Specifically, we observe the driven dynamics for 100 ps and apply the condition  $\min(|\psi|/|\psi_0|) < 10^{-3}$  to determine unstable states. We note that the heating regime has a similar shape as the parameter set for which no stable solutions can be found by applying the harmonic balance method with ten harmonics [31, 36].

Within our analytical solution for the optical conductivity in Eq. (3), we have determined an upper boundary for the driving frequency of  $\sqrt{3}\omega_H$  for the enhancement effect to occur. At this boundary, the second term in the denominator of Eq. (3) switches sign. Our simulations confirm this prediction for  $\omega_H < \omega_J$ . However, as

visible in Fig. 3, an additional suppression lowers this upper bound for superconductors with  $\omega_J < (\sqrt{3}-1)\omega_H$ . Here, the enhancement regime is approximately limited by the resonance frequency of the time crystalline state at  $\omega_{\text{dr}} = \omega_H + \omega_J$  [17]. This modified upper bound derives from higher-order terms not included in the analytical solution.

Finally, we consider cuprates with  $\omega_H < \omega_J < \sqrt{3}\omega_H$ . In this case, the previous suppression of interlayer transport for  $\omega_{\text{dr}} \approx \omega_J$  switches to strong enhancement, as exemplified in Fig. 2(b). Therefore, we propose to drive these particular systems near the plasma frequency  $\omega_J$ . In typical monolayer cuprates, such as LSCO, the superconducting gap  $2\Delta$  is larger than the Josephson plasma energy  $\hbar\omega_J$  [37–39]. At low temperatures, the Higgs frequency approximately equals  $2\Delta/\hbar$  [27, 40], so it is larger than the Josephson plasma frequency in these materials, i.e.,  $\omega_J < \omega_H$ . However, while the temperature dependence of the Higgs mode in cuprate superconductors is the subject of debate [25, 26], the case  $\omega_H < \omega_J < \sqrt{3}\omega_H$  might be realized for higher temperatures. For these temperatures, stronger damping and thermal fluctuations might suppress or reduce the enhancement mechanism. This regime will be discussed elsewhere. Further decay channels of the Higgs mode have been studied in Refs. [41, 42].

In conclusion, we propose a novel mechanism for light-enhanced interlayer transport in cuprate superconductors by optically exciting Higgs oscillations which induce parametric amplification of the superconducting response. Both our analytical and numerical calculations show that the superconducting response of a monolayer cuprate is significantly amplified when the optical driving is slightly blue-detuned from the Higgs frequency. Since our calculations demonstrate a significant Higgs-mediated enhancement of interlayer transport for a broad regime of driving parameters at  $T = 0$ , we propose to verify this effect first for low temperatures; higher temperatures will be discussed elsewhere. The enhancement mechanism presented in this work is broadly applicable to cuprate superconductors because it does not rely on the existence of suitable phonons but is mediated by Higgs oscillations of the Cooper pair condensate itself. Therefore it constitutes light control of a functionality of high-temperature superconductors that utilizes the intrinsic mode structure of these materials and their nonlinear coupling.

This work is supported by the Deutsche Forschungsgemeinschaft (DFG) in the framework of SFB 925 and the Cluster of Excellence “Advanced Imaging of Matter” (EXC 2056), Project No. 390715994. J.O. acknowledges support by the Georg H. Endress Foundation.



- 
- [1] D. Fausti, R. I. Tobey, N. Dean, S. Kaiser, A. Dienst, M. C. Hoffmann, S. Pyon, T. Takayama, H. Takagi, and A. Cavalleri, Light-induced superconductivity in a stripe-ordered cuprate, *Science* **331**, 189 (2011).
- [2] M. Buzzi, D. Nicoletti, M. Fechner, N. Tancogne-Dejean, M. A. Sentef, A. Georges, T. Biesner, E. Uykur, M. Dreschel, A. Henderson, T. Siegrist, J. A. Schlueter, K. Miyagawa, K. Kanoda, M.-S. Nam, A. Ardavan, J. Coulthard, J. Tindall, F. Schlawin, D. Jaksch, and A. Cavalleri, Photomolecular high-temperature superconductivity, *Phys. Rev. X* **10**, 031028 (2020).
- [3] M. Budden, T. Gebert, M. Buzzi, G. Jotzu, E. Wang, T. Matsuyama, G. Meier, Y. Laplace, D. Pontiroli, M. Riccò, F. Schlawin, D. Jaksch, and A. Cavalleri, Evidence for metastable photo-induced superconductivity in  $\text{K}_3\text{C}_{60}$ , arXiv e-prints (2020), [arXiv:2002.12835 \[cond-mat.supr-con\]](#).
- [4] W. Hu, S. Kaiser, D. Nicoletti, C. R. Hunt, I. Gierz, M. C. Hoffmann, M. Le Tacon, T. Loew, B. Keimer, and A. Cavalleri, Optically enhanced coherent transport in  $\text{YBa}_2\text{Cu}_3\text{O}_{6.5}$  by ultrafast redistribution of interlayer coupling, *Nat. Mater.* **13**, 705 (2014).
- [5] S. Kaiser, C. R. Hunt, D. Nicoletti, W. Hu, I. Gierz, H. Y. Liu, M. Le Tacon, T. Loew, D. Haug, B. Keimer, and A. Cavalleri, Optically induced coherent transport far above  $T_c$  in underdoped  $\text{YBa}_2\text{Cu}_3\text{O}_{6+\delta}$ , *Phys. Rev. B* **89**, 184516 (2014).
- [6] M. Först, A. Frano, S. Kaiser, R. Mankowsky, C. R. Hunt, J. J. Turner, G. L. Dakovski, M. P. Minitti, J. Robinson, T. Loew, M. Le Tacon, B. Keimer, J. P. Hill, A. Cavalleri, and S. S. Dhesi, Femtosecond x rays link melting of charge-density wave correlations and light-enhanced coherent transport in  $\text{YBa}_2\text{Cu}_3\text{O}_{6.6}$ , *Phys. Rev. B* **90**, 184514 (2014).
- [7] K. A. Cremin, J. Zhang, C. C. Homes, G. D. Gu, Z. Sun, M. M. Fogler, A. J. Millis, D. N. Basov, and R. D. Averitt, Photoenhanced metastable c-axis electrodynamics in stripe-ordered cuprate  $\text{La}_{1.885}\text{Ba}_{0.115}\text{CuO}_4$ , *Proc. Natl. Acad. Sci. USA* **116**, 19875 (2019).
- [8] R. Mankowsky, A. Subedi, M. Först, S. O. Mariager, M. Chollet, H. T. Lemke, J. S. Robinson, J. M. Glowina, M. P. Minitti, A. Frano, M. Fechner, N. A. Spaldin, T. Loew, B. Keimer, A. Georges, and A. Cavalleri, Non-linear lattice dynamics as a basis for enhanced superconductivity in  $\text{YBa}_2\text{Cu}_3\text{O}_{6.5}$ , *Nature* **516**, 71 (2014).
- [9] S. J. Denny, S. R. Clark, Y. Laplace, A. Cavalleri, and D. Jaksch, Proposed parametric cooling of bilayer cuprate superconductors by terahertz excitation, *Phys. Rev. Lett.* **114**, 137001 (2015).
- [10] R. Höppner, B. Zhu, T. Rexin, A. Cavalleri, and L. Mathey, Redistribution of phase fluctuations in a periodically driven cuprate superconductor, *Phys. Rev. B* **91**, 104507 (2015).
- [11] Z. M. Raines, V. Stanev, and V. M. Galitski, Enhancement of superconductivity via periodic modulation in a three-dimensional model of cuprates, *Phys. Rev. B* **91**, 184506 (2015).
- [12] A. A. Patel and A. Eberlein, Light-induced enhancement of superconductivity via melting of competing bond-density wave order in underdoped cuprates, *Phys. Rev. B* **93**, 195139 (2016).
- [13] J.-i. Okamoto, A. Cavalleri, and L. Mathey, Theory of enhanced interlayer tunneling in optically driven high- $T_c$  superconductors, *Phys. Rev. Lett.* **117**, 227001 (2016).
- [14] J.-i. Okamoto, W. Hu, A. Cavalleri, and L. Mathey, Transiently enhanced interlayer tunneling in optically driven high- $T_c$  superconductors, *Phys. Rev. B* **96**, 144505 (2017).
- [15] S. Rajasekaran, E. Casandruc, Y. Laplace, D. Nicoletti, G. D. Gu, S. R. Clark, D. Jaksch, and A. Cavalleri, Parametric amplification of a superconducting plasma wave, *Nat. Phys.* **12**, 1012 (2016).
- [16] F. Schlawin, A. S. D. Dietrich, M. Kiffner, A. Cavalleri, and D. Jaksch, Terahertz field control of interlayer transport modes in cuprate superconductors, *Phys. Rev. B* **96**, 064526 (2017).
- [17] G. Homann, J. G. Cosme, and L. Mathey, Higgs time crystal in a high- $T_c$  superconductor, *Phys. Rev. Research* **2**, 043214 (2020).
- [18] T. Koyama and M. Tachiki, I-V characteristics of Josephson-coupled layered superconductors with longitudinal plasma excitations, *Phys. Rev. B* **54**, 16183 (1996).
- [19] D. van der Marel and A. A. Tsvetkov, Transverse-optical Josephson plasmons: Equations of motion, *Phys. Rev. B* **64**, 024530 (2001).
- [20] T. Koyama, Josephson plasma resonances and optical properties in high- $T_c$  superconductors with alternating junction parameters, *J. Phys. Soc. Jpn.* **71**, 2986 (2002).
- [21] M. Harland, S. Brener, A. I. Lichtenstein, and M. I. Katsnelson, Josephson lattice model for phase fluctuations of local pairs in copper oxide superconductors, *Phys. Rev. B* **100**, 024510 (2019).
- [22] D. Dulić, A. Pimenov, D. van der Marel, D. M. Broun, S. Kamal, W. N. Hardy, A. A. Tsvetkov, I. M. Sutjaha, R. Liang, A. A. Menovsky, A. Loidl, and S. S. Saxena, Observation of the transverse optical plasmon in  $\text{SmLa}_{0.8}\text{Sr}_{0.2}\text{CuO}_{4-\delta}$ , *Phys. Rev. Lett.* **86**, 4144 (2001).
- [23] H. Shibata and T. Yamada, Double Josephson plasma resonance in  $T^*$  phase  $\text{SmLa}_{1-x}\text{Sr}_x\text{CuO}_{4-\delta}$ , *Phys. Rev. Lett.* **81**, 3519 (1998).
- [24] D. N. Basov and T. Timusk, Electrodynamics of high- $T_c$  superconductors, *Rev. Mod. Phys.* **77**, 721 (2005).
- [25] K. Katsumi, N. Tsuji, Y. I. Hamada, R. Matsunaga, J. Schneeloch, R. D. Zhong, G. D. Gu, H. Aoki, Y. Gallais, and R. Shimano, Higgs mode in the  $d$ -wave superconductor  $\text{Bi}_2\text{Sr}_2\text{CaCu}_2\text{O}_{8+x}$  driven by an intense terahertz pulse, *Phys. Rev. Lett.* **120**, 117001 (2018).
- [26] H. Chu, M.-J. Kim, K. Katsumi, S. Kovalev, R. D. Dawson, L. Schwarz, N. Yoshikawa, G. Kim, D. Putzky, Z. Z. Li, H. Raffy, S. Germanskiy, J.-C. Deinert, N. Awari, I. Ilyakov, B. Green, M. Chen, M. Bawatna, G. Christiani, G. Logvenov, Y. Gallais, A. V. Boris, B. Keimer, A. P. Schnyder, D. Manske, M. Gensch, Z. Wang, R. Shimano, and S. Kaiser, Phase-resolved Higgs response in superconducting cuprates, *Nat. Commun.* **11**, 1793 (2020).
- [27] R. Shimano and N. Tsuji, Higgs mode in superconductors, *Annu. Rev. Condens. Matter Phys.* **11**, 103 (2020).
- [28] C. M. Varma, Higgs boson in superconductors, *J. Low Temp. Phys.* **126**, 901 (2002).
- [29] D. Pekker and C. Varma, Amplitude/Higgs modes in condensed matter physics, *Annu. Rev. Condens. Matter Phys.* **6**, 269 (2015).
- [30] Z. Sun, M. M. Fogler, D. N. Basov, and A. J. Millis, Collective modes and terahertz near-field response of su-

- perconductors, *Phys. Rev. Research* **2**, 023413 (2020).
- [31] See Supplemental Material for simulation parameters, the derivation of the analytical prediction in Eq. (3), a comparison between the quadratic and fully nonlinear models, and a stability analysis by the harmonic balance method.
- [32] V. L. Ginzburg and L. D. Landau, On the theory of superconductivity, *Zh. Eksp. Teor. Fiz.* **20**, 1064 (1950).
- [33] J. B. Kogut, An introduction to lattice gauge theory and spin systems, *Rev. Mod. Phys.* **51**, 659 (1979).
- [34] K. Yee, Numerical solution of initial boundary value problems involving maxwell's equations in isotropic media, *IEEE Trans. Antennas Propag.* **14**, 302 (1966).
- [35] L. D. Landau and E. M. Lifšic, *Mechanics*, 3rd ed. (Butterworth-Heinemann, Oxford, 1976).
- [36] J. C. Slater, Mousai: An open-source general purpose harmonic balance solver (13th ASME Dayton Engineering Sciences Symposium, Dayton, Ohio, USA, 2017).
- [37] S. V. Dordevic, S. Komiya, Y. Ando, and D. N. Basov, Josephson plasmon and inhomogeneous superconducting state in  $\text{La}_{2-x}\text{Sr}_x\text{CuO}_4$ , *Phys. Rev. Lett.* **91**, 167401 (2003).
- [38] G. Deutscher, Coherence and single-particle excitations in the high-temperature superconductors, *Nature* **397**, 410 (1999).
- [39] M. Hashimoto, T. Yoshida, K. Tanaka, A. Fujimori, M. Okusawa, S. Wakimoto, K. Yamada, T. Kakeshita, H. Eisaki, and S. Uchida, Distinct doping dependences of the pseudogap and superconducting gap of  $\text{La}_{2-x}\text{Sr}_x\text{CuO}_4$  cuprate superconductors, *Phys. Rev. B* **75**, 140503 (2007).
- [40] F. Yang and M. W. Wu, Theory of Higgs modes in  $d$ -wave superconductors, *Phys. Rev. B* **102**, 014511 (2020).
- [41] F. Peronaci, M. Schiró, and M. Capone, Transient dynamics of  $d$ -wave superconductors after a sudden excitation, *Phys. Rev. Lett.* **115**, 257001 (2015).
- [42] Y. Murakami, P. Werner, N. Tsuji, and H. Aoki, Damping of the collective amplitude mode in superconductors with strong electron-phonon coupling, *Phys. Rev. B* **94**, 115126 (2016).

# Supplemental Material for Higgs-mediated enhancement of interlayer transport in high- $T_c$ superconductors

Guido Homann,<sup>1</sup> Jayson G. Cosme,<sup>1,2,3</sup> Junichi Okamoto,<sup>4,5</sup> and Ludwig Mathey<sup>1,2</sup>

<sup>1</sup>*Zentrum für Optische Quantentechnologien and Institut für Laserphysik, Universität Hamburg, 22761 Hamburg, Germany*

<sup>2</sup>*The Hamburg Centre for Ultrafast Imaging, Luruper Chaussee 149, 22761 Hamburg, Germany*

<sup>3</sup>*National Institute of Physics, University of the Philippines, Diliman, Quezon City 1101, Philippines*

<sup>4</sup>*Institute of Physics, University of Freiburg, Hermann-Herder-Strasse 3, 79104 Freiburg, Germany*

<sup>5</sup>*EUCOR Centre for Quantum Science and Quantum Computing,  
University of Freiburg, Hermann-Herder-Strasse 3, 79104 Freiburg, Germany*

## CONTENTS

I. Simulation parameters	2
II. Analytical derivation of the Higgs-mediated enhancement of interlayer transport	2
III. Comparison between the quadratic and fully nonlinear models	4
IV. Stability analysis by the harmonic balance method	4
References	5

## I. SIMULATION PARAMETERS

Table I summarizes the parameters of the monolayer cuprate superconductors studied in the main text. Our parameter choice of  $\mu$  and  $g$  implies an equilibrium condensate density  $n_0 = \mu/g = 2 \times 10^{21} \text{ cm}^{-3}$  at  $T = 0$ . The capacitive coupling constant is given by

$$\alpha = \frac{\epsilon_z \epsilon_0}{8K n_0 e^2 d_z^2} = 1, \quad (1)$$

For the  $c$ -axis plasma frequency, we consider the three cases  $\omega_J/2\pi = 2 \text{ THz}$ ,  $\omega_J/2\pi = 9 \text{ THz}$ , and  $\omega_J/2\pi = 15 \text{ THz}$ . The Higgs frequency is fixed at  $\omega_H/2\pi = 6 \text{ THz}$ .

TABLE I. Model parameters used in the simulations.

$K \text{ (meV}^{-1}\text{)}$	$1.38 \times 10^{-5}$
$\mu \text{ (meV)}$	$4.24 \times 10^{-3}$
$g \text{ (meV } \text{\AA}^3\text{)}$	2.12
$\gamma/2\pi \text{ (THz)}$	0.5
$d_z \text{ (\AA)}$	10
$t_z \text{ (meV)}$	$9.44 \times 10^{-4}, 1.91 \times 10^{-2}, 5.31 \times 10^{-2}$

## II. ANALYTICAL DERIVATION OF THE HIGGS-MEDIATED ENHANCEMENT OF INTERLAYER TRANSPORT

Here, we consider a monolayer cuprate superconductor at zero temperature. Since the system is driven along the  $c$  axis, it exhibits no in-plane dynamics. Additionally, we employ periodic boundary conditions so that the cuprate can be described by the two following equations of motion:

$$\ddot{a} + \gamma \dot{a} + \omega_J^2 \sin(a)(1+h)^2 = j, \quad (2)$$

$$\ddot{h} + \gamma \dot{h} + \omega_H^2 \left( h + \frac{3}{2}h^2 + \frac{1}{2}h^3 \right) + 2\alpha\omega_J^2 [1 - \cos(a)](1+h) = 0. \quad (3)$$

Neglecting all nonlinear terms except for the quadratic coupling between the Higgs field  $h$  and the unitless vector potential  $a$ , we find

$$\ddot{a} + \gamma \dot{a} + \omega_J^2 a + 2\omega_J^2 a h = j, \quad (4)$$

$$\ddot{h} + \gamma \dot{h} + \omega_H^2 h + \alpha\omega_J^2 a^2 = 0, \quad (5)$$

as in Ref. [1]. Now, we expand  $j$ ,  $a$ , and  $h$  in the form

$$f = f^{(0)} + \lambda f^{(1)} + \lambda^2 f^{(2)} + \lambda^3 f^{(3)} + \mathcal{O}(\lambda^4), \quad (6)$$

where  $\lambda \ll 1$  is a small expansion parameter. We take the current  $j$  induced by driving and probing as

$$j^{(1)} = j_{\text{dr},1} e^{-i\omega_{\text{dr}} t} + j_{\text{pr},1} e^{-i\omega_{\text{pr}} t} + \text{c.c.} \quad (7)$$

Hence, there are no zeroth order contributions and we obtain

$$a^{(1)} = a_{\text{dr},1} e^{-i\omega_{\text{dr}} t} + a_{\text{pr},1} e^{-i\omega_{\text{pr}} t} + \text{c.c.}, \quad (8)$$

$$h^{(1)} = 0 \quad (9)$$

in first order, where

$$a_{\text{dr},1} = \frac{j_{\text{dr},1}}{\omega_J^2 - \omega_{\text{dr}}^2 - i\gamma\omega_{\text{dr}}}, \quad (10)$$

$$a_{\text{pr},1} = \frac{j_{\text{pr},1}}{\omega_J^2 - \omega_{\text{pr}}^2 - i\gamma\omega_{\text{pr}}}. \quad (11)$$



In second order, we have

$$a^{(2)} = 0, \quad (12)$$

$$h^{(2)} = h_0 + h_1 e^{-2i\omega_{\text{dr}} t} + h_2 e^{-2i\omega_{\text{pr}} t} + h_3 e^{-i(\omega_{\text{dr}} - \omega_{\text{pr}})t} + h_4 e^{-i(\omega_{\text{dr}} + \omega_{\text{pr}})t} + \text{c.c.}, \quad (13)$$

where

$$h_0 = -\frac{2\alpha\omega_{\text{J}}^2}{\omega_{\text{H}}^2} (|a_{\text{dr},1}|^2 + |a_{\text{pr},1}|^2), \quad (14)$$

$$h_1 = \frac{\alpha\omega_{\text{J}}^2 a_{\text{dr},1}^2}{4\omega_{\text{dr}}^2 - \omega_{\text{H}}^2 + 2i\gamma\omega_{\text{dr}}}, \quad (15)$$

$$h_2 = \frac{\alpha\omega_{\text{J}}^2 a_{\text{pr},1}^2}{4\omega_{\text{pr}}^2 - \omega_{\text{H}}^2 + 2i\gamma\omega_{\text{pr}}}, \quad (16)$$

$$h_3 = \frac{2\alpha\omega_{\text{J}}^2 a_{\text{dr},1} a_{\text{pr},1}^*}{(\omega_{\text{dr}} - \omega_{\text{pr}})^2 - \omega_{\text{H}}^2 + i\gamma(\omega_{\text{dr}} - \omega_{\text{pr}})}, \quad (17)$$

$$h_4 = \frac{2\alpha\omega_{\text{J}}^2 a_{\text{dr},1} a_{\text{pr},1}}{(\omega_{\text{dr}} + \omega_{\text{pr}})^2 - \omega_{\text{H}}^2 + i\gamma(\omega_{\text{dr}} + \omega_{\text{pr}})}. \quad (18)$$

In third order, we find the following correction for the vector potential at the probing frequency:

$$a_{\text{pr},3} = \frac{2\omega_{\text{J}}^2 (h_0 a_{\text{pr},1} + h_2 a_{\text{pr},1}^* + h_3^* a_{\text{dr},1} + h_4 a_{\text{dr},1}^*)}{\omega_{\text{pr}}^2 - \omega_{\text{J}}^2 + i\gamma\omega_{\text{pr}}}. \quad (19)$$

Using  $\omega_{\text{pr}} \ll \omega_{\text{dr}}, \omega_{\text{H}}, \omega_{\text{J}}$  and  $|j_{\text{pr},1}| < |j_{\text{dr},1}|$ , we can neglect the term  $h_2 a_{\text{pr},1}^*$  and simplify the denominators of Eqs. (11), (17) and (18):

$$\begin{aligned} a_{\text{pr},3} &\approx \frac{4\alpha\omega_{\text{J}}^2 |a_{\text{dr},1}|^2 a_{\text{pr},1}}{\omega_{\text{H}}^2} \left( 1 - \frac{2\omega_{\text{H}}^2}{\omega_{\text{dr}}^2 - \omega_{\text{H}}^2 + i\gamma\omega_{\text{dr}}} \right) \\ &= \frac{4\alpha |j_{\text{dr},1}|^2 j_{\text{pr},1} (\omega_{\text{dr}}^2 - 3\omega_{\text{H}}^2 + i\gamma\omega_{\text{dr}})}{\omega_{\text{H}}^2 (\omega_{\text{dr}}^2 - \omega_{\text{H}}^2 + i\gamma\omega_{\text{dr}}) [(\omega_{\text{dr}}^2 - \omega_{\text{J}}^2)^2 + \gamma^2 \omega_{\text{dr}}^2]}. \end{aligned} \quad (20)$$

Thus, we obtain

$$\begin{aligned} \omega_{\text{pr}} \sigma(\omega_{\text{pr}}) &= \frac{i\epsilon_z \epsilon_0 j(\omega_{\text{pr}})}{a(\omega_{\text{pr}})} \\ &= \frac{i\epsilon_z \epsilon_0 \lambda j_{\text{pr}}}{\lambda a_{\text{pr},1} + \lambda^3 a_{\text{pr},3}} \\ &\approx \frac{i\epsilon_z \epsilon_0 \omega_{\text{J}}^2 \omega_{\text{H}}^2 (\omega_{\text{dr}}^2 - \omega_{\text{H}}^2 + i\gamma\omega_{\text{dr}}) [(\omega_{\text{dr}}^2 - \omega_{\text{J}}^2)^2 + \gamma^2 \omega_{\text{dr}}^2]}{\omega_{\text{H}}^2 (\omega_{\text{dr}}^2 - \omega_{\text{H}}^2 + i\gamma\omega_{\text{dr}}) [(\omega_{\text{dr}}^2 - \omega_{\text{J}}^2)^2 + \gamma^2 \omega_{\text{dr}}^2] + 4\alpha\omega_{\text{J}}^2 |j_{\text{dr}}|^2 (\omega_{\text{dr}}^2 - 3\omega_{\text{H}}^2 + i\gamma\omega_{\text{dr}})}, \end{aligned} \quad (21)$$

with the original driving amplitude  $j_{\text{dr}} = \lambda j_{\text{dr},1}$ . Taking  $j_{\text{dr}} = 0$  leads to the equilibrium solution

$$\omega_{\text{pr}} \sigma(\omega_{\text{pr}}) \approx i\epsilon_z \epsilon_0 \omega_{\text{J}}^2. \quad (22)$$

### III. COMPARISON BETWEEN THE QUADRATIC AND FULLY NONLINEAR MODELS

We refer to Eqs. (4) and (5) as the quadratic model, which approximates the fully nonlinear model given by Eqs. (2) and (3). In Fig. 1, we investigate the effect of the approximation on the effective interlayer coupling. We also compare the numerical results for the two models to the analytical prediction from the previous section. While the analytical prediction shows excellent agreement with the numerical results for the quadratic model, simulating the fully nonlinear model leads to slightly different results, even for weak driving.

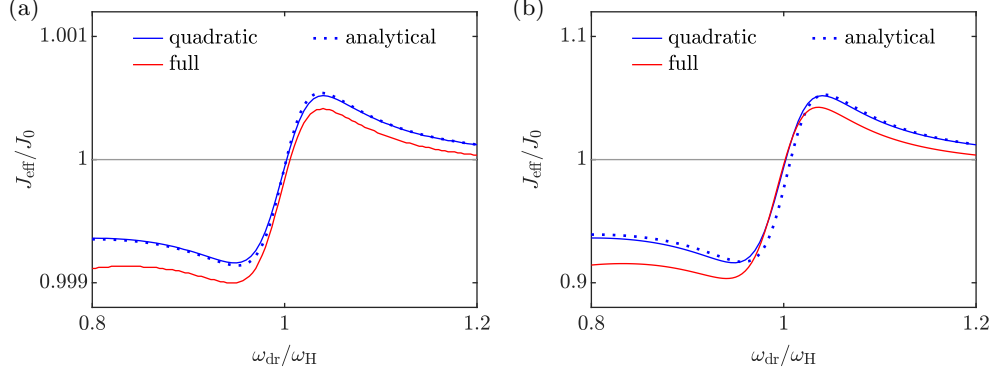


FIG. 1. Effective interlayer coupling for the quadratic and fully nonlinear models. The driving amplitudes are  $E_0 = 10 \text{ kV cm}^{-1}$  in (a) and  $E_0 = 100 \text{ MV cm}^{-1}$  in (b). The dotted lines indicate the analytical predictions based on the quadratic model.

### IV. STABILITY ANALYSIS BY THE HARMONIC BALANCE METHOD

In this section, we discuss the dynamical stability of the Higgs field and the vector potential using the harmonic balance method. Given a set of nonlinear ordinary differential equations with periodically changing parameters, the harmonic balance method maps the problem into an algebraic one by expanding solutions by multiple harmonics. The obtained algebraic equation is solved by the Newton or secant method. In order to solve the fully nonlinear equations of motion (2) and (3), we use the Krylov-Newton method with ten harmonics in Mousai [2].

In Fig. 2, we plot the absolute value of the time-averaged Higgs field for various driving frequencies  $\omega_{\text{dr}}$  and amplitudes  $E_0$  (corresponding to Fig. 3 in the main text). Due to the nonlinearity of the equation of motion, the system may show multistability; the obtained solution depends on the initial condition. Here, at each frequency, we sweep from weak to strong driving using the preceding calculation as the initial condition for the next calculation. We confirm the stability of the obtained solutions by adding slight noise to the initial conditions.

The blank area corresponds to the case where the Krylov-Newton method fails to obtain periodic steady solutions. The strong instability appears around  $\omega_{\text{dr}} \simeq \omega_J$  and  $\omega_H/2$ , which agrees with the numerical solutions in the main text. The harmonic balance method overestimates the instability regimes due the difficulty of solving nonlinear algebraic equations accurately. At higher frequencies near  $\omega_H$ , we find that the multistability is more prominent, and that

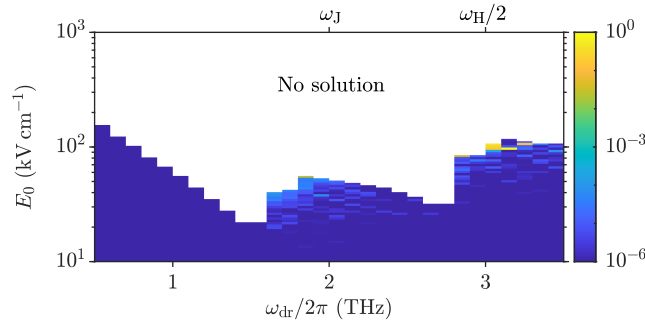


FIG. 2. Absolute value of the time-averaged Higgs field as a function of driving frequency and field strength, as obtained by the harmonic balance method with ten harmonics.

the instability needs large driving amplitude. This regime corresponds to the heating regime identified via spectral entropy or depletion. The deviation between the harmonic balance method and the numerical solutions may come from the fact that chaotic solutions cannot be obtained by the harmonic balance method due to its harmonic ansatz.

- 
- [1] G. Homann, J. G. Cosme, and L. Mathey, Higgs time crystal in a high- $T_c$  superconductor, [Phys. Rev. Research \*\*2\*\*, 043214 \(2020\)](#).
  - [2] J. C. Slater, Mousai: An open-source general purpose harmonic balance solver (13th ASME Dayton Engineering Sciences Symposium, Dayton, Ohio, USA, 2017).